



Scholars Research Library

Der Pharma Chemica, 2015, 7(8):265-275
(<http://derpharmachemica.com/archive.html>)



ISSN 0975-413X
CODEN (USA): PCHHAX

Corrosion inhibition of mild steel by new N-heterocyclic compound in 1 M HCl: Experimental and computational study

Y. ELouadi¹, F. Abridach¹, A. Bouyanzer¹, R. Touzani^{1,2}, O. Riant³, B. ElMahi¹,
A. El Assyry⁴, S. Radi¹, A. Zarrouk¹ and B. Hammouti¹

¹LCAE-URAC18, Faculty of Science, University of Mohammed Premier, Oujda, Morocco

²Faculté Pluridisciplinaire de Nador, Université Mohammed Premier, Selouane 62700, Nador, Morocco

³Institute of Condensed Matter and Nanosciences (IMCN) Molecules, Solids and Reactivity (MOST). Université Catholique de Louvain, Louvain-la-Neuve, Belgium

⁴Laboratoire d'Optoélectronique et de Physico-chimie des Matériaux, (Unité associée au CNRST), Université Ibn Tofail, Faculté des Sciences, Kénitra, Morocco

ABSTRACT

The aim of this study is to investigate the inhibition efficiency of N^1, N^1, N^5, N^5 -tetrakis((3,5-dimethyl-1H-pyrazol-1-yl)methyl)naphthalene-1,5-diamine (BF5), for mild steel corrosion in 1.0 M HCl solution. For this purpose, weight loss, electrochemical impedance spectroscopy and potentiodynamic measurements were realized. The effect of BF5 on the mild steel corrosion was also studied by quantum chemical calculations. Increasing inhibitor concentration led to significant reduction in the corrosion rate of mild steel, with inhibitor efficiency value above 97%. The corrosion behavior of steel in 1.0 M HCl without and with the inhibitor at various concentrations was studied at the temperature range of 308 - 343 K. Potentiodynamic polarization showed that this inhibitor as mixed-type inhibitor. The Nyquist plots showed that increasing BF5 concentration, charge-transfer resistance increased and double-layer capacitance decreased, involving increased inhibition efficiency. The adsorption of BF5 on the mild steel surface was well described by the Langmuir adsorption model.

Keywords: Mild steel, Acid medium, Corrosion, Weight loss, Electrochemical techniques, DFT.

INTRODUCTION

Mild steel finds application in a wide spectrum of industries, owing to its high mechanical strength, abundance and low cost. Corrosion, like an insidious cancer, deteriorates the surface of the metals and alloys in different environment. In industries, acid solutions are more frequently used in boilers for descaling, pickling, etc. Mild steel suffers from severe corrosive attack in this acidic condition. Hence, the study on corrosion of mild steel in aggressive acidic condition assumes significance from industrial point of view.

The use of chemical inhibitors is one of the most practiced methods for protecting against corrosion, especially in acid media, to prevent metal dissolution and acid consumption [1]. Various organic and non-organic compounds have been studied as inhibitors to protect metals from corrosion. Usually, organic compounds exert a significant influence on metal surface adsorption and therefore can be used as effective corrosion inhibitors. The efficiency of these organic corrosion inhibitors is related to the presence of polar functions containing S, O or N atoms which are centers for the establishment of the adsorption process [2-26].

Theoretical chemistry, including quantum chemical calculation has been proved to be a very powerful tool for studying the mechanism of corrosion inhibition [27]. This theoretical approach has been widely used to investigate a

correlation between molecule structure and inhibition efficiency of an organic compound [28,29]. Therefore, it is worthwhile to compute the structural parameters including the highest occupied molecular orbital energy (E_{HOMO}), the lowest unoccupied molecular orbital (E_{LUMO}), dipole moment (μ), atomic charge, etc.

In the present work, the corrosion inhibition efficiency of new N-heterocyclic derivative (BF5) on mild steel in 1.0 M hydrochloric acid solution was studied using weight loss measurement, potentiodynamic polarization curves and electrochemical impedance spectroscopy (EIS). Effects of inhibitor concentration and temperature on inhibition action were investigated. The quantum chemical parameters from the inhibitor molecule to iron were calculated using density functional theory (DFT) at B3LYP/6-31G(d,p) level. The chemical structure of inhibitor was given in Fig. 1.

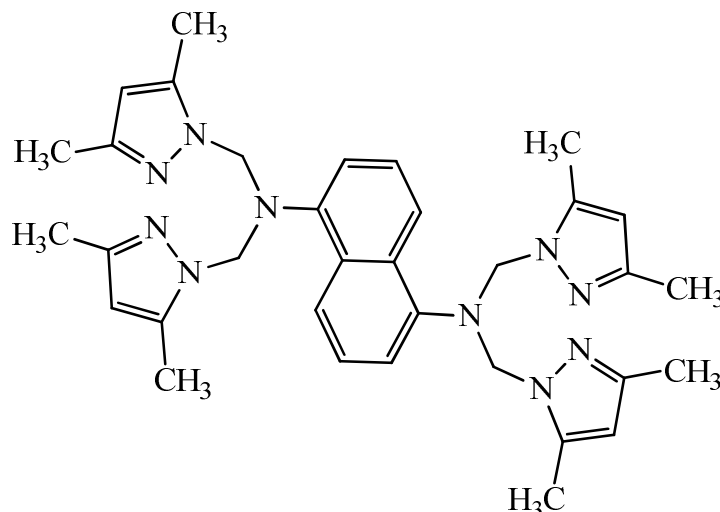


Figure 1: N^1,N^1,N^5,N^5 -tetrakis((3,5-dimethyl-1H-pyrazol-1-yl)methyl)naphthalene-1,5-diamine (BF5)

MATERIALS AND METHODS

Materials

The steel used in this study is a mild steel with a chemical composition (in wt%) of 0.09% P, 0.01 % Al, 0.38 % Si, 0.05 % Mn, 0.21 % C, 0.05 % S and the remainder iron (Fe). The steel samples were pre-treated prior to the experiments by grinding with amery paper sic (220, 400, 800, 1000 and 1200); rinsed with distilled water, degreased in acetone, washed again with bidistilled water and then dried at room temperature before use.

Solutions

The aggressive solutions of 1.0 M HCl were prepared by dilution of analytical grade 37% HCl with distilled water. The concentration range of N^1,N^1,N^5,N^5 -tetrakis((3,5-dimethyl-1H-pyrazol-1-yl)methyl)naphthalene-1,5-diamine (BF5) used was 10^{-5} M to 10^{-3} M.

Gravimetric study

Gravimetric experiments were performed according to the standard methods [30], the mild steel sheets of $1 \times 1 \times 0.1$ cm were abraded with a series of emery papers SiC (120, 600 and 1200) and then washed with distilled water and acetone. After weighing accurately, the specimens were immersed in a 100 mL beaker containing 250 mL of 1.0 M HCl solution with and without addition of different concentrations inhibitor. All the aggressive acid solutions were open to air. After 6 h of acid immersion, the specimens were taken out, washed, dried, and weighed accurately. In order to get good reproducibility, all measurements were performed few times and average values were reported to obtain good reproducibility. The inhibition efficiency ($\eta_{\text{WL}}\%$) and surface coverage (θ) were calculated as follows:

$$C_R = \frac{W_b - W_a}{At} \quad (1)$$

$$\eta_{\text{WL}} (\%) = \left(1 - \frac{w_i}{w_0} \right) \times 100 \quad (2)$$

where W_b and W_a are the specimen weight before and after immersion in the tested solution, w_0 and w_i are the values of corrosion weight losses of mild steel in uninhibited and inhibited solutions, respectively, A the total area of the mild steel specimen (cm^2) and t is the exposure time (h).

Electrochemical measurements

The electrochemical measurements were carried out using Volta lab (Tacussel- Radiometer PGZ 100) potentiostat and controlled by Tacussel corrosion analysis software model (Voltmaster 4) at under static condition. The corrosion cell used had three electrodes. The reference electrode was a saturated calomel electrode (SCE). A platinum electrode was used as auxiliary electrode of surface area of 1 cm². The working electrode was mild steel of the surface 0.32 cm². All potentials given in this study were referred to this reference electrode. The working electrode was immersed in test solution for 30 min to a establish steady state open circuit potential (E_{ocp}). After measuring the E_{ocp} , the electrochemical measurements were performed. All electrochemical tests have been performed in aerated solutions at 308 K. The EIS experiments were conducted in the frequency range with high limit of 100 kHz and different low limit 0.1 Hz at open circuit potential, with 10 points per decade, at the rest potential, after 30 min of acid immersion, by applying 10 mV ac voltage peak-to-peak. Nyquist plots were made from these experiments. The best semicircle can be fit through the data points in the Nyquist plot using a non-linear least square fit so as to give the intersections with the x -axis.

The inhibition efficiency of the inhibitor was calculated from the charge transfer resistance values using the following equation:

$$\eta_z \% = \frac{R_{ct}^i - R_{ct}^\circ}{R_{ct}^i} \times 100 \quad (3)$$

Where, R_{ct}° and R_{ct}^i are the charge transfer resistance in absence and in presence of inhibitor, respectively.

After ac impedance test, the potentiodynamic polarization measurements of mild steel substrate in inhibited and uninhibited solution were scanned from cathodic to the anodic direction, with a scan rate of 1 mV s⁻¹. The potentiodynamic data were analysed using the polarization VoltaMaster 4 software. The linear Tafel segments of anodic and cathodic curves were extrapolated to corrosion potential to obtain corrosion current densities (I_{corr}). From the polarization curves obtained, the corrosion current (I_{corr}) was calculated by curve fitting using the equation:

$$I = I_{corr} \left[\exp\left(\frac{2.3\Delta E}{\beta_a}\right) - \exp\left(\frac{2.3\Delta E}{\beta_c}\right) \right] \quad (4)$$

The inhibition efficiency was evaluated from the measured I_{corr} values using the following relationship:

$$\eta_{Tafel}(\%) = \frac{I_{corr} - I_{corr(i)}}{I_{corr}} \times 100 \quad (5)$$

where I_{corr} and $I_{corr(i)}$ are the corrosion current densities for steel electrode in the uninhibited and inhibited solutions, respectively.

Quantum chemical calculations

Complete geometry optimization of the inhibitor molecules were performed using density functional theory (DFT) with Beck's three-parameter exchange functional along with LeeYangeParr non-local correlation functional (B3LYP) with 6-1G* basis set using the Gaussian 03 programme package [31]. Frontier molecular orbitals (HOMO and LUMO) were used to interpret the adsorption of inhibitor molecules on the metal surface. According to DFT-Koopman's theorem [32,33], the ionization potential (I) is approximated as the negative of the highest occupied molecular orbital energy (E_{HOMO}) and the negative of the lowest unoccupied molecular orbital energy (E_{LUMO}) is related to the electron affinity (A).

$$I = -E_{HOMO} \quad (6)$$

$$A = -E_{LUMO} \quad (7)$$

Natural bond orbital (NBO) analysis [34] was performed to evaluate the electron density distributions. The electron density plays an important role in calculating the chemical reactivity parameters. The global reactivities include electronegativity (χ), global hardness (η) and the global softness (σ). They can be calculated from the following equations:

$$\chi = \frac{I + A}{2} \quad (8)$$

$$\eta = \frac{I - A}{2} \quad (9)$$

$$\sigma = \frac{1}{\eta} = -\frac{2}{E_{HOMO} - E_{LUMO}} \quad (10)$$

RESULTS AND DISCUSSION

Potentiodynamic polarization study

Polarization measurements were undertaken to investigate the behavior of mild steel electrode in 1.0 M HCl in the absence and presence of inhibitor. The current-potential relationship for the mild steel electrode in various test solutions is shown in Fig. 2 while the electrochemical data obtained from the polarization curves are presented in Table 1.

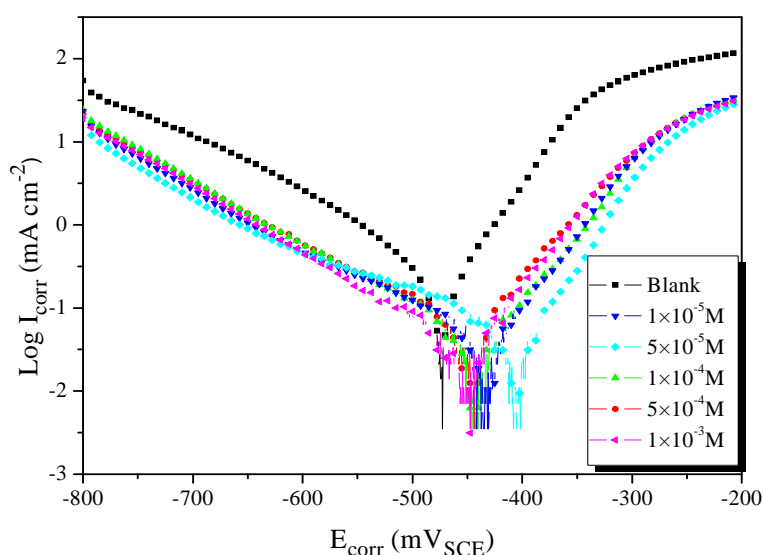


Figure 2: Polarization curves of mild steel in 1.0 M HCl containing different concentrations of BF5

Table 1: The electrochemical parameters for mild steel in 1.0 M HCl solution without and with different concentration of BF5 at 308 K

Inhibitor	Conc (M)	$-E_{corr}$ (mV/SCE)	β_a (mV dec ⁻¹)	$-\beta_c$ (mV dec ⁻¹)	I_{corr} ($\mu\text{A cm}^{-2}$)	η_{Tafel} (%)
HCl	1.0	450	67.1	144.2	361.8	—
T1	1×10^{-5}	440	65.0	138.9	44.2	87.8
	5×10^{-5}	440	72.1	137.8	42.4	88.3
	1×10^{-4}	430	63.6	154.7	39.9	89.0
	5×10^{-4}	410	56.2	112.8	30.5	91.6
	1×10^{-3}	440	56.0	119.5	22.4	93.8

Fig. 2 represents that both anodic and cathodic current densities decreased in the presence of the investigated compound. This decrease is more pronounced with the growth in inhibitor concentration. This observation demonstrates that the inhibitor is adsorbed on the mild steel surface. Consequently, this adsorption reduces both anodic dissolution of iron at anodic sites and cathodic evolution of hydrogen at cathodic sites. As the inhibitor concentration rises, the extent of adsorption increases, leading to increased inhibition efficiency.

Comparing the samples without and with inhibitor, it is obviously that when BF5 is used as inhibitor, the E_{corr} values for mild steel in 1.0 M HCl shift slightly toward more positive direction from that for the uninhibited sample (Figure 2, Table 1). If the change in E_{corr} value was more than 85 mV, a chemical compound could be recognized as an

anodic or a cathodic type inhibitor [35]. The maximum shift in E_{corr} was 40 mV towards anodic direction indicating mixed mode of corrosion with predominately anodic effect.

Compared with the blank experiment, both the cathodic and anodic Tafel slope changed slightly which implied that the cathodic hydrogen evolution and anodic metal dissolved reaction had been compressed.

Electrochemical impedance spectroscopic study

Nyquist plots of mild steel in 1.0 M HCl solution without and with different concentrations of BF5 are shown in Fig. 3, respectively. It is seen that the Nyquist diagram shows a capacitive loop, which suggests that the corrosion of mild steel in test solution is mainly controlled by charge transfer process [36,37]. The diameter of the capacitive loop in the presence of inhibitor is bigger than that in the uninhibited solution and increases with the inhibitor concentrations. The impedance parameter such as charge transfer resistance (R_{ct}), double layer capacitance (C_{dl}), the frequency (f_{max}) and inhibition efficiency are listed in Tables 2 for BF5.

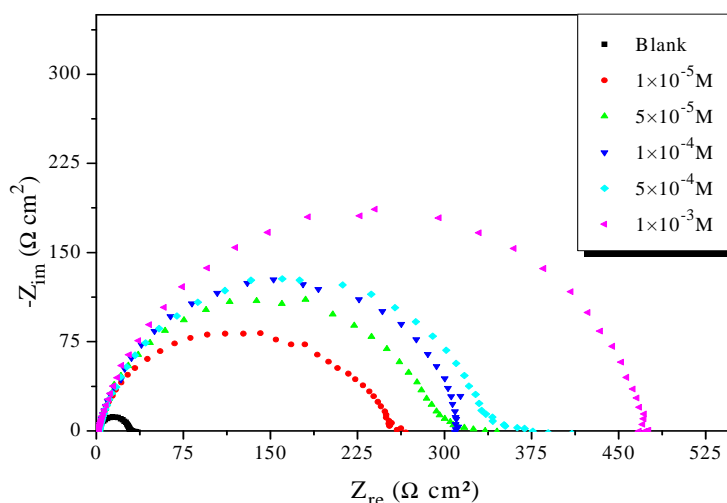


Figure 3: Nyquist plot for steel in 1M HCl solution containing different concentrations of BF5

Table 2. EIS parameters for the corrosion of mild steel in 1.0 M HCl containing BF5 at 308 K

Inhibitor	Conc (M)	R_{ct} ($\Omega \text{ cm}^2$)	f_{max} (Hz)	C_{dl} ($\mu\text{F cm}^{-2}$)	η_{z} (%)
HCl	1.0	27.4	100	58.0	—
BF5	1×10^{-5}	242.4	12.5	52.5	88.7
	5×10^{-5}	291.3	12.5	43.7	90.6
	1×10^{-4}	314.0	12.5	40.5	91.3
	5×10^{-4}	334.5	12.5	38.1	91.8
	1×10^{-3}	472.3	10	33.7	94.2

It is seen that the R_{ct} value increases and the C_{dl} value decreases by the addition of inhibitor. A large charge transfer resistance (R_{ct}) is associated with a slower corroding system. An increase in charge transfer resistance values could be ascribed to the adsorption of inhibitor at steel-acid interface, which effectively blocked the active sites on mild steel surface and hence enhances the corrosion resistance of mild steel in acidic medium. The decrease in C_{dl} values with an increase in the inhibitor concentration, suggesting that either thickness of protective layer increased, or local dielectric constant of film decreased, or both occurred simultaneously [38]. The inhibition efficiency increases with increasing inhibitor concentration due to more and more coverage of mild steel surface with the inhibitor concentrations. The inhibition efficiencies calculated from EIS showed the same trend as those obtained from potentiodynamic polarization (Tables 1 and 2).

Weight loss study

Effect of inhibitor concentration

Table 1 shows the results obtained from weight loss measurements for mild steel in 1.0 M HCl solutions in the absence and presence of different concentrations of BF5. It has been observed from the results that the η_{WL} of BF5 increases from 88.6% to 97.4% with the increase in inhibitor concentration from 10^{-5} to 10^{-3} M. Indeed, corrosion rate values of mild steel decreases from 0.036 to 0.008 $\text{mg/cm}^2 \text{ h}$ on the addition of 10^{-5} to 10^{-3} M of BF5. The increase in efficiency from 88.6% to 97.4% may be due to the blocking effect of the surface by

both adsorption and film formation mechanisms, which decreases the effective area of corrosion attack [39]. The results confirm that BF5 is an efficient corrosion inhibitor, which gives efficiency values as high as 97.4% in room temperature. The inhibiting performance exhibited by the compound may be due to the presence of protonated form of nitrogen atoms of the compound which makes it adsorb quickly on the mild steel surface, thus forming an insoluble stable film on the surface of the mild steel. It is clear that BF5 showed good inhibition for mild steel corrosion in 1.0 M HCl solutions because the inhibitor molecule is made of planar aromatic rings of pyrazole and a benzene ring and also contains N atoms and π -electrons [40].

Table 3. Weight loss values of various concentrations of BF5 in 1.0 M HCl solution

Medium	Conc (K)	C_R (mg/cm ² h)	θ	η_{WL} (%)
Blank	1.0	0.320	—	—
	1×10^{-5}	0.036	0.886	88.6
	5×10^{-5}	0.029	0.909	90.9
BF5	1×10^{-4}	0.025	0.922	92.2
	5×10^{-4}	0.015	0.954	95.4
	1×10^{-3}	0.008	0.974	97.4

Adsorption isotherm

The extent of adsorption of an inhibitor on the metal surface is usually influenced by the parameters such as the nature, chemical structure, distribution of charge on the molecule and charge on the metal. Basic information regarding the nature of interaction of the adsorbed inhibitor molecule and the mild steel surface can be elucidated using adsorption isotherm. The surface coverage θ can be obtained by using the well-known formula $\eta_{WL}\%/100$. The value of θ increased with increase in inhibitor concentration, demonstrating the more pronounced adsorption of inhibitor on the metal surface. The θ value was fitted to various isotherms like Langmuir, Freundlich, Temkin and Frumkin. Langmuir was found to give the best description on the adsorption of inhibitor. The equation corresponding to Langmuir adsorption isotherm is

$$\frac{C_{inh}}{\theta} = \frac{1}{K} + C_{inh} \quad (11)$$

where C_{inh} represents the concentration of the inhibitor in mol/L and K denotes the adsorption-desorption equilibrium constant. A plot of C_{inh} vs C_{inh}/θ gave a straight line with a slope around unity (Fig. 4). This suggests monolayer adsorption of inhibitor on the surface of mild steel. The values of thermochemical parameters such as K , ΔG_{ads}° and the correlation coefficient R^2 were enumerated in Table 4.

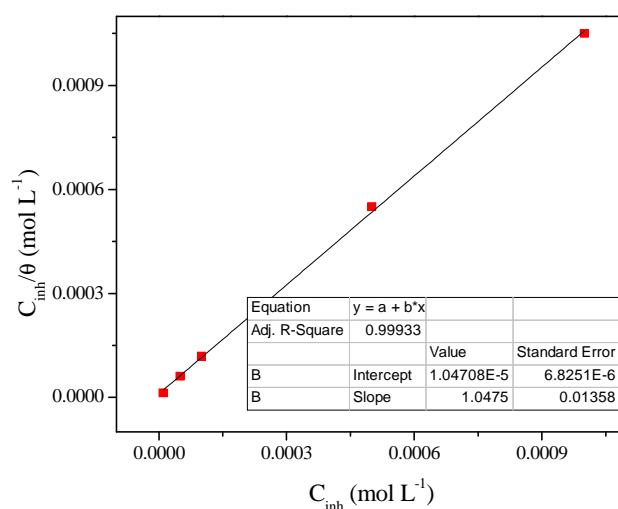


Figure 4: The langmuir adsorption isotherm plots for the adsorption of BF5 in 1.0 M HCl on the surface of mild steel

Table 4. Thermodynamic parameters for mild steel in 1.0 M HCl in the presence of inhibitor at 308 K

	Slope	R ²	K _{ads} (L mol ⁻¹)	ΔG _{ads} ^o (KJ/mol)
PHQ	1.05	0.99933	95503.67	-39.65

ΔG_{ads}^o calculated from the slope of Langmuir adsorption isotherm using the following equation:

$$\Delta G_{ads}^{\circ} = -RT \ln(55.5 K_{ads}) \quad (12)$$

where R is gas constant and T is absolute temperature of experiment and the constant value of 55.5 is the concentration of water in solution in mol L⁻¹. In Fig. 4, the intercept on the vertical axis is the value of 1/K_{ads}, which is 1.04708×10⁻⁵ M. Generally, values of ΔG_{ads}^o up to -20 kJ/mol, the types of adsorption were regarded as physisorption, the inhibition acts due to the electrostatic interactions between the charged molecules and the charged metal, while values around -40 kJ/mol or smaller are associated with chemisorption as a result of sharing or transfer of electrons from organic molecules to the metal surface to form a coordinate type of bond (chemisorption) [41]. Then according to Eq. (12), we calculated the ΔG_{ads}^o = -39.65 kJ/mol. Therefore it can be concluded that the adsorption of the BF5 on the mild steel surface is mainly the chemical adsorption inevitably accompanied by the physical adsorption.

Influence of Temperature

The loss in the weight of the steel samples in 1.0 M HCl in the absence and presence of various concentrations of BF5 at different temperatures was determined. The effect of temperature on the inhibition efficiency of the BF5 is shown in Table 5. In all cases, an increase in BF5 concentration leads to a decrease in the corrosion rate of samples indicating that the presence of BF5 retards the general corrosion of samples in 1.0 M HCl. On the other hand, an increase in temperature from 313-343 K resulted in an increase in the corrosion rate for all the concentration of BF5, probably as a result of desorption of inhibitor molecules from the metal surface.

Table 5. Weight loss values of BF5 at various temperatures in 1.0 M HCl solution

Medium	Temp (K)	C _R (mg/cm ² h)	θ	η _{wL} (%)
Blank	313	1.300	—	—
	323	1.828	—	—
	333	3.635	—	—
	343	6.336	—	—
TEA	313	0.075	0.942	94.2
	323	0.173	0.906	90.6
	333	0.408	0.888	88.8
	343	1.265	0.800	80.0

Thermodynamic parameters are important to understand the inhibition mechanism. The thermodynamic functions for dissolution of mild steel without and with the addition of optimum concentration of BF5 at various temperatures were calculated from the logarithm of corrosion rate (C_R) of metal in acidic HCl solution by using the Arrhenius equation:

$$\ln C_R = \frac{E_a}{RT} + A \quad (13)$$

where C_R is the corrosion rate, E_a is the apparent activation energy, and A is the preexponential factor. The arrhenius plots of Ln C_R versus 1/T for the blank and optimum concentration of BF4 give a straight line and a slope equal to -E_a/R shown in Figure 5, from which the values of E_a for the inhibited corrosion reaction of mild steel have been calculated and recorded in Table 6.

In 1.0 M HCl solution, the addition of BF5 leads to an increase in the apparent activation energy to value greater than that of the uninhibited solution. The results show that the addition of BF5 decreases metal dissolution in 1.0 M HCl medium. On the other hand, the increase in the apparent activation energy may be interpreted as physical adsorption that occurs in the first stage [42]. Szauer and Brand explained that the increase in activation energy can be attributed to an appreciable decrease in the adsorption of the inhibitor on the mild steel surface with increase in temperature.

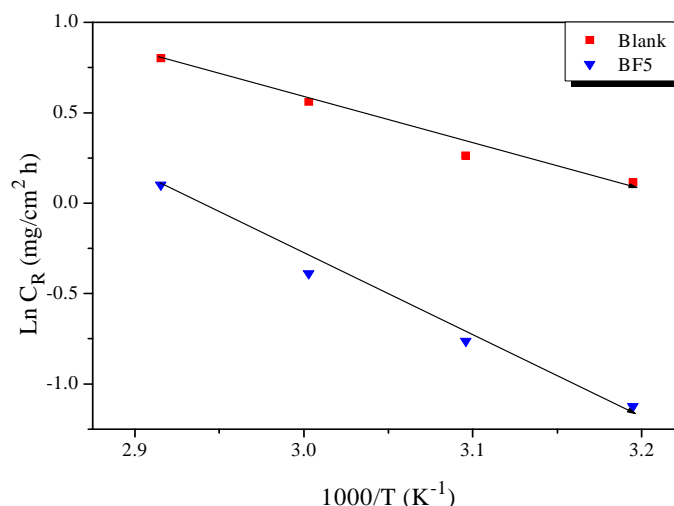


Figure 5: Arrhenius plots for mild steel corrosion rates $\text{Ln}(C_R)$ versus $1/T$ in 1.0 M HCl in absence and in presence of optimum concentration of BF5

In order to calculate activation parameters for the corrosion process, an alternative formulation of Arrhenius (14) was used:

$$C_R = \frac{RT}{Nh} \exp\left(\frac{\Delta S_a}{R}\right) \exp\left(\frac{\Delta H_a}{RT}\right) \quad (14)$$

where C_R is the corrosion rate, h is the Plank's constant, N is the Avogadro's number, the enthalpy of activation (ΔH_a), and the entropy of activation (ΔS_a). Fig. 6 shows a representative plot for the transition state in 1.0 M HCl solutions without and with of 10^{-3} M of BF5. Activation parameters obtained from these graphs are given in Table 6.

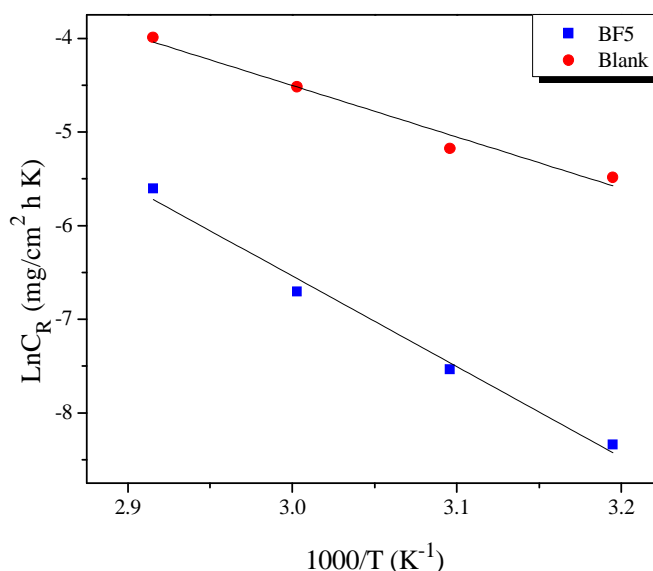


Figure 6: Transition-state plots for mild steel corrosion rates $\text{Ln}(C_R/T)$ versus $1/T$ in 1.0 M HCl in absence and in presence of optimum concentrations of BF5

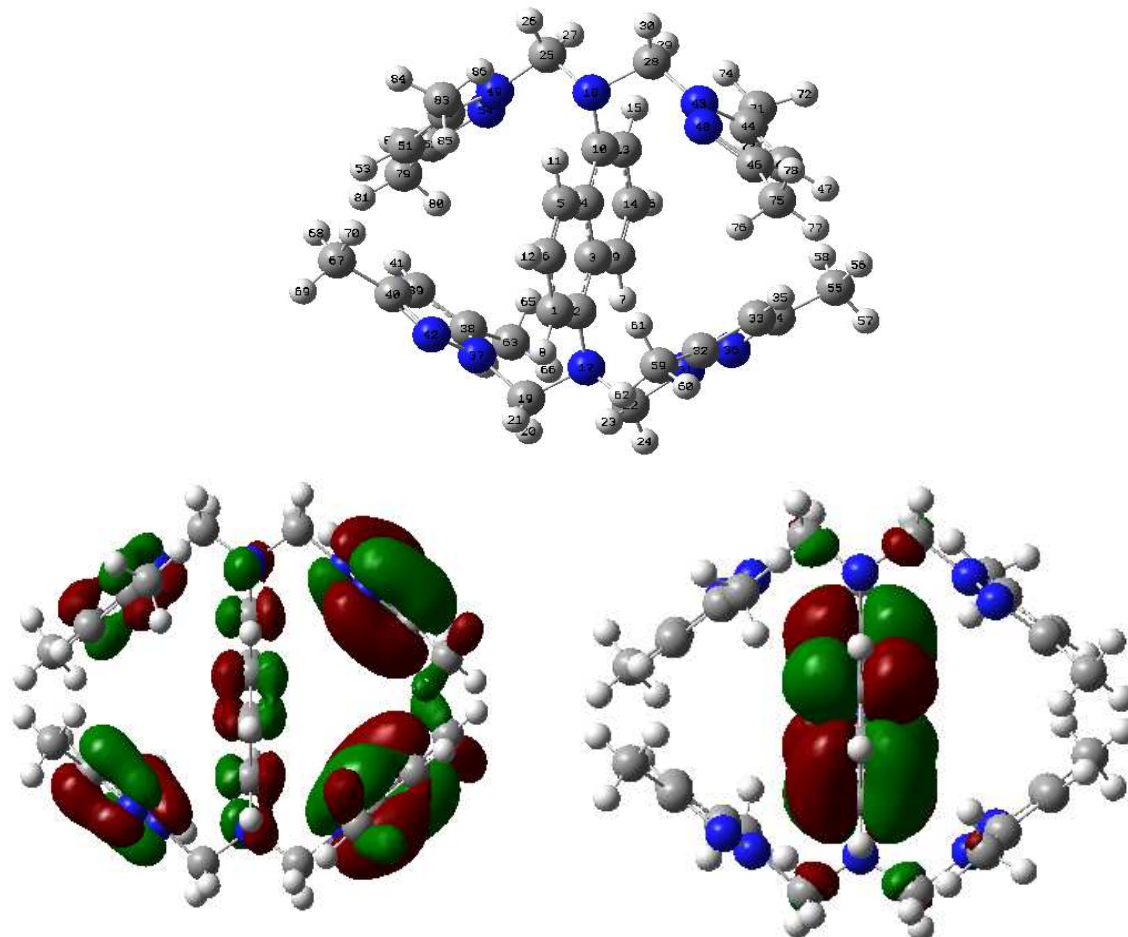
Table 6. The values of activation parameters for mild steel in 1.0 M HCl in the absence and presence of 10^{-3} M of BF5

Conc (M)	E_a (kJ mol ⁻¹)	ΔH_a (kJ mol ⁻¹)	ΔS_a (J mol ⁻¹ K ⁻¹)
Blank	48.40	45.68	-97.95
BF5	83.11	80.38	-10.75

The thermodynamic parameters (ΔH_a and ΔS_a) of the dissolution reaction of steel in 1.0 M HCl in the presence of BF5 is higher than that of in the absence of inhibitor (blank). The positive signs of the enthalpies ΔH_a reflect the endothermic nature of the steel dissolution process and mean that the dissolution of steel is difficult [43]. In the presence of BF5, the increase of ΔS_a reveals that an increase in disordering takes place on going from reactants to the activated complex [44].

Quantum chemical studies

Fig.7 represents the optimized geometry, HOMO, LUMO orbital of the inhibitor molecule in the combined form. Quantum chemical parameters are given in Table 7. It is well known that HOMO is often associated with the electron donating ability of a molecule, whereas LUMO indicates its ability to accept electrons [45]. Reportedly, excellent corrosion inhibitors are usually those organic compounds which not only offer electrons to unoccupied orbital of the metal, but also accept free electrons from the metal [46]. From Fig. 7, it can be seen that in the combined form of inhibitor molecules, the HOMO location is mainly distributed on the BF5 molecule and LUMO location is distributed on the two rings benzene. This indicates that electrons are transferred from the orbital of BF5 to the metal. Electrons in the occupied orbital of metal are transferred to the LUMO of the BF5 molecule.

**Figure 7:** Optimized geometry, HOMO and LUMO of the inhibitor molecule in the combined form

The value of highest occupied molecular orbital, E_{HOMO} indicates the tendency of the molecule to donate electrons to acceptor molecule with empty and low energy orbital. Therefore, the energy of the lowest unoccupied molecular orbital, E_{LUMO} indicates the tendency of the molecule to accept electrons [47]. The energy gap ΔE is an important parameter which is related to reactivity of the inhibitor molecule towards the metal surface. The interaction of inhibitor molecule to the metal surface is related to transfer of electrons from inhibitor to metal surface. Polarity of a

covalent bond (Dipole moment μ) can be understood by distribution of electrons in a molecule and large value of dipole moment μ favour the adsorption of inhibitor.

Table 7. Quantum chemical parameters for BF5

Quantum parameters	P1
E_{HOMO} (eV)	-8.6260
E_{LUMO} (eV)	-5.7144
ΔE gap (eV)	2.9116
μ (debye)	0.2114
$I = -E_{HOMO}$ (eV)	8.6260
$A = -E_{LUMO}$ (eV)	5.7144
$\chi = \frac{I + A}{2}$ (eV)	7.1702
$\eta = \frac{I - A}{2}$ (eV)	1.4558
$\sigma = \frac{1}{\eta}$	0.6869
TE (eV)	-50201.1386

Absolute hardness and softness are important properties to measure the molecular stability and reactivity. It is apparent that the chemical hardness fundamentally signifies the resistance towards the deformation or polarization of the electron cloud of the atoms, ions or molecules under small perturbation of chemical reaction. A hard molecule has a large energy gap and a soft molecule has a small energy gap [48]. In our present work the studied molecule has low hardness value 1.4558 (eV) and a highest value of softness of 0.6869

The total energy calculated by quantum chemical methods is equal to -50201.1386 eV. Hohenberg and Kohn [49] proved that the total energy of a system including that of the many body effects of electrons (exchange and correlation) in the presence of static external potential (for example, the atomic nuclei) is a unique functional of the charge density. The minimum value of the total energy functional is the ground state energy of the system. The electronic charge density which yields this minimum is then the exact single particle ground state energy.

CONCLUSION

All the measurements showed that the BF5 has excellent inhibition properties against the mild steel corrosion in hydrochloric acid solution. Inhibition efficiency of this inhibitor decreases with increase in temperature and further it leads to an increase in activation energy. The inhibitor follows the Langmuir adsorption isotherm in the process of adsorption. EIS measurements also indicates that the inhibitor performance increase due to the adsorption of molecule on the metal surface. Potentiodynamic polarization measurements showed that the inhibitor acts as mixed type of inhibitor. The inhibitor showed maximum inhibition efficiency at 1.0 mM concentration of the studied inhibitor. The inhibition efficiency of BF5 as corrosion inhibitor indicates that their inhibition effects are closely related to E_{HOMO} , E_{LUMO} , hardness, dipole moment and total energy. The inhibition efficiencies determined by EIS, potentiodynamic polarization and weight loss studies are in good agreement.

REFERENCES

- [1] M. Lashgari, M.R. Arshadi, S. Miandari, *Electrochim. Acta* **2010**, 55, 6058.
- [2] B. Xu, W. Yang, Y. Liu, X. Yin, W. Gong, Y. Chen, *Corros. Sci.* **2014**, 78, 260.
- [3] M. Prajila, J. Sam, J. Bincy, J. Abraham, *J. Mater. Environ. Sci.* **2012**, 3, 1045.
- [4] U.J. Naik, V.A. Panchal, A.S. Patel, N.K. Shah, *J. Mater. Environ. Sci.*, **2012**, 3, 935.
- [5] A.H. Al Hamzi, H. Zarrok, A. Zarrouk, R. Salghi, B. Hammouti, S.S. Al-Deyab, M. Bouachrine, A. Amine, F. Guenoun, *Int. J. Electrochem. Sci.*, **2013**, 8, 2586.
- [6] A. Zarrouk, B. Hammouti, H. Zarrok, I. Warad, M. Bouachrine, *Der Pharm. Chem.*, **2011**, 3, 263.
- [7] D. Ben Hmamou, R. Salghi, A. Zarrouk, M. Messali, H. Zarrok, M. Errami, B. Hammouti, Lh. Bazzi, A. Chakir, *Der Pharm. Chem.*, **2012**, 4, 1496.

- [8] A. Ghazoui, N. Benaht, S.S. Al-Deyab, A. Zarrouk, B. Hammouti, M. Ramdani, M. Guenbour, *Int. J. Electrochem. Sci.*, **2013**, 8, 2272.
- [9] A. Zarrouk, H. Zarrok, R. Salghi, N. Bouroumane, B. Hammouti, S.S. Al-Deyab, R. Touzani, *Int. J. Electrochem. Sci.*, **2012**, 7, 10215.
- [10] H. Bendaha, A. Zarrouk, A. Aouniti, B. Hammouti, S. El Kadiri, R. Salghi, R. Touzani, *Phys. Chem. News*, **2012**, 64, 95.
- [11] S. Rekkab, H. Zarrok, R. Salghi, A. Zarrouk, Lh. Bazzi, B. Hammouti, Z. Kabouche, R. Touzani, M. Zougagh, *J. Mater. Environ. Sci.*, **2012**, 3, 613.
- [12] A. Zarrouk, B. Hammouti, H. Zarrok, M. Bouachrine, K.F. Khaled, S.S. Al-Deyab, *Int. J. Electrochem. Sci.*, **2012**, 6, 89.
- [13] A. Mansri, B. Bouras, *Mor. J. Chem.*, **2014**, 2, 252.
- [14] H. Zarrok, K. Al Mamari, A. Zarrouk, R. Salghi, B. Hammouti, S. S. Al-Deyab, E. M. Essassi, F. Bentiss, H. Oudda, *Int. J. Electrochem. Sci.*, **2012**, 7, 10338.
- [15] H. Zarrok, A. Zarrouk, R. Salghi, Y. Ramli, B. Hammouti, M. Assouag, E. M. Essassi, H. Oudda and M. Taleb, *J. Chem. Pharm. Res.*, **2012**, 4, 5048.
- [16] A. Zarrouk, B. Hammouti, A. Dafali, F. Bentiss, *Ind. Eng. Chem. Res.* **2013**, 52, 2560.
- [17] H. Zarrok, A. Zarrouk, R. Salghi, H. Oudda, B. Hammouti, M. Assouag, M. Taleb, M. Ebn Touhami, M. Bouachrine, S. Boukhris, *J. Chem. Pharm. Res.* **2012**, 4, 5056.
- [18] H. Zarrok, H. Oudda, A. El Midaoui, A. Zarrouk, B. Hammouti, M. Ebn Touhami, A. Attayibat, S. Radi, R. Touzani, *Res. Chem. Intermed.* **2012**, 38, 2051.
- [19] A. Ghazoui, A. Zarrouk, N. Benaht, R. Salghi, M. Assouag, M. El Hezzat, A. Guenbour, B. Hammouti, *J. Chem. Pharm. Res.* **2014**, 6, 704.
- [20] A. Fouda, A. El-bendary, M. Diabb, A. Bakra, *Mor. J. Chem.*, **2014**, 2, 302.
- [21] A. Zarrouk, H. Zarrok, R. Salghi, R. Touir, B. Hammouti, N. Benchat, L.L. Afrine, H. Hannache, M. El Hezzat, M. Bouachrine, *J. Chem. Pharm. Res.* **2013**, 5, 1482.
- [22] H. Zarrok, A. Zarrouk, R. Salghi, M. Assouag, B. Hammouti, H. Oudda, S. Boukhris, S.S. Al Deyab, I. Warad, *Der Pharm. Lett.* **2013**, 5, 43.
- [23] D. Ben Hmamou, M.R. Aouad, R. Salghi, A. Zarrouk, M. Assouag, O. Benali, M. Messali, H. Zarrok, B. Hammouti, *J. Chem. Pharm. Res.* **2012**, 4, 3498.
- [24] M. Belayachi, H. Serrar, H. Zarrok, A. El Assyry, A. Zarrouk, H. Oudda, S. Boukhris, B. Hammouti, Eno E. Ebenso, A. Geunbour, *Int. J. Electrochem. Sci.* **2015**, 10, 3010.
- [25] H. Tayebi, H. Bourazmi, B. Himmi, A. El Assyry, Y. Ramli, A. Zarrouk, A. Geunbour, B. Hammouti, Eno E. Ebenso, *Der Pharm. Lett.* **2014**, 6(6), 20.
- [26] H. Tayebi, H. Bourazmi, B. Himmi, A. El Assyry, Y. Ramli, A. Zarrouk, A. Geunbour, B. Hammouti, *Der Pharm. Chem.* **2014**, 6(5), 220.
- [27] G. Gece, *Corros. Sci.* **2008**, 50, 2981.
- [28] V.V. Torres, V.A. Rayol, M. Magalhaes, G.M. Viana, L.C.S. Aguiar, S.P. Machado, H. Orofino, E. D'Elia, *Corros. Sci.* **2014**, 79, 108.
- [29] S. Issaadi, T. Douadi, S. Chafaa, *Appl. Surf. Sci.* **2014**, 316, 582.
- [30] ASTM, G 31-72, American Society for Testing and Materials, Philadelphia, PA, **1990**.
- [31] Gaussian 03, Revision B.01, M. J. Frisch, et al., Gaussian, Inc., Pittsburgh, PA, **2003**.
- [32] W.J. Hehre, L. Radom, P.v.R. Schleyer, A.J. Pople, *Wiley-Interscience*, New York, **1986**.
- [33] J.F. Janak, *Phys. Rev. B* **1978**, 18, 7165.
- [34] R. Stowasser, R. Hoffmann, *J. Am. Chem. Soc.* **1999**, 121, 3414.
- [35] K.R. Ansari, M.A. Quraishi, A. Singh, *Corros. Sci.* **2014**, 79, 5.
- [36] W. Yang, W.J. Mortier, *J. Am. Chem. Soc.* **1986**, 108, 5708.
- [37] A. Döner, R. Solmaz, M. Özcan, G. Kardaş, *Corros. Sci.* **2011**, 53, 2902.
- [38] E. McCafferty, N. Hackerman, *J. Electrochem. Soc.* **1972**, 119, 146.
- [39] T. P. Zhao, G.N. Mu, *Corros. Sci.* **1999**, 41, 1937.
- [40] I. Ahamed, M. A. Quraishi, *Corros. Sci.* **2010**, 52, 651.
- [41] Z. Szklarskasmialowska, J. Mankowski, *Corros. Sci.* **1978**, 18, 953.
- [42] S. Martinez, I. Stern, *Appl. Surf. Sci.* **2002**, 199, 83.
- [43] Guan N.M., Xueming L., Fei L., *Mater. Chem. Phys.* **2004**, 86, 59.
- [44] E. Khamis, A. Hosney, S. El-Khodary, *Afinidad* **1995**, 52, 95.
- [45] F. Zhang, Y. Tang, Z. Cao, W. Jing, Z. Wu, Y. Chen, *Corros. Sci.* **2012**, 61, 1.
- [46] P. Zhao, Q. Liang, Y. Li, *Appl. Surf. Sci.* **2005**, 252, 1596.
- [47] I. Ahamad, R. Prasad, M. A. Quraishi, *J. Solid State Electrochem.* **2010**, 14, 2095.
- [48] G. Gece, S. Bilgic, *Corros. Sci.*, **2009**, 51, 1876.
- [49] H. Ju, Z.P. Kai, Y. Li, *Corros. Sci.*, **2008**, 50, 865.